Bifunctional Oxygen Reduction

International Edition: DOI: 10.1002/anie.201504369
German Edition: DOI: 10.1002/ange.201504369

Oxygen Reduction with a Bifunctional Iridium Dihydride Complex

Christoph Schiwek, Jenni Meiners, Moritz Förster, Christian Würtele, Martin Diefenbach, Max C. Holthausen, and Sven Schneider**

Dedicated to Professor Tobin J. Marks on the occasion of his 70th birthday

Abstract: *The iridium dihydride $[Ir(H)_2(HPNP)]^+$ ($PNP = N(CH_2CH_2PtBu_2)_2$) reacts with O_2 to give the unusual, square-planar iridium(III) hydroxide $[Ir(OH)(PNP)]^+$ and water. Regeneration of the dihydride with H_2 closes a quasi-catalytic synthetic oxygen-reduction reaction (ORR) cycle that can be run several times. Experimental and computational examinations are in agreement with an oxygenation mechanism via rate-limiting O_2 coordination followed by H-transfer at a single metal site, facilitated by the cooperating pincer ligand. Hence, the four electrons required for the ORR are stored within the two covalent M–H bonds of a mononuclear metal complex.*

The direct use of O_2 for selective oxidation is a key goal for sustainable catalysis. Besides synthetic transformations, the oxygen-reduction reaction (ORR: $O_2 + 4H^+ + 4e^- \rightarrow 2H_2O$) is pivotal for biological and technical processes of energy conversion, such as respiration and fuel cell applications. However, the ORR imposes particular challenges: 1) The four electrons required have to be provided by multiple redox centers. Side reactions, such as two-electron H_2O_2 formation, can reduce catalytic efficiency or result in undesired oxidation products. Nature typically uses multinuclear transition-metal cofactors and redox non-innocent ligands.[1] 2) The ORR requires the delivery of four protons. This has been taken into account in catalyst design, for example, by tethering of acidic groups in the proximity of the oxygen-reducing site.[2]

The Rauchfuss group reported an ORR within a synthetic cycle, catalyzed by a bifunctional iridium catalyst (Scheme 1a).[2a,3] This remarkable system combines both aspects, that is, a cooperating amine ligand and electron delivery from the metal hydride bond rather than the metal ion which does not change its formal oxidation state (Ir^{III}).[4] Most recently, Milstein and co-workers also reported oxygen reduction to a hydroxide making use of metal–ligand cooperation.[5] However, monohydrides like **1** provide only two redox equivalents and the ORR was proposed to proceed via a putative hydroperoxide intermediate,[6] which reacts with a second equivalent of **1**. Direct four-electron O_2 reduction might be accessible with dihydrido complexes. Support is provided by Goldberg's group, who reported the formation of hydroxide **3** (Scheme 1) from the reaction of dihydride **4** with O_2, albeit only in minor amounts within a product mixture of mostly peroxo complexes, such as **5**.[7]

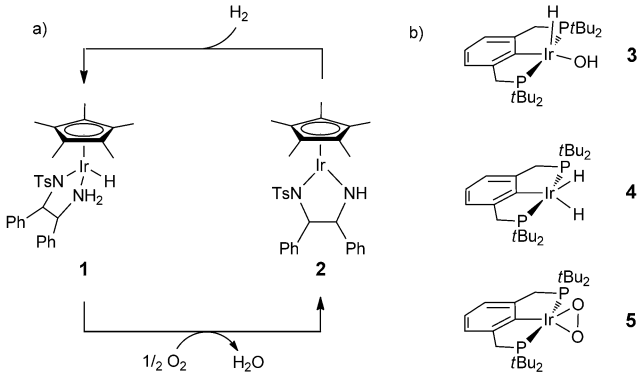

Scheme 1. a) ORR with a bifunctional Ir hydride complex.[2a] b) Ir pincer complexes examined in the context of O_2 reduction.[7]

Here, we examine the ORR with an iridium(III) dihydride amine complex. O_2 splitting affords an unusual, square-planar iridium(III) hydroxide. The full ORR is completed upon H_2 heterolysis. Experimental and computational examinations suggest a mononuclear mechanism.

$[Ir(H)_2(HPNP)]PF_6$ (**6**; $HPNP = HN(CH_2CH_2PtBu)_2$) is obtained in good yield by reaction of in situ generated $[Ir(COE)(HPNP)]PF_6$ (COE = cyclooctene)[8] with H_2. Complex **6** is stable in THF. In CH_2Cl_2 at room temperature (RT) the hydride ligands are slowly replaced by chloride over several hours. NMR characterization of **6** is in agreement with a square-pyramidal configuration with one hydride in apical position. The two hydrides are resolved at low T (−47.1 and −16.0 ppm) and exhibit rapid exchange at RT on the NMR timescale ($\Delta^{\ddagger}H = 9.6 \pm 0.2$ kcal mol^{-1}, $\Delta^{\ddagger}S = 2.4 \pm 0.5$ cal mol^{-1} K^{-1}; CD_2Cl_2). The molecular structure of **6** could not be derived by X-ray diffraction but crystallization from acetonitrile gave suitable crystals of $[Ir(H)_2(NCMe)(HPNP)]PF_6$ (**7**, see the Supporting Information). In an H_2 atmosphere, **6** forms the polyhydride $[Ir(H)_2(H_2)(HPNP)]PF_6$ (**8**), which in turn eliminates H_2 upon solvent evaporation (Scheme 2 and Supporting Information).

[*] M. Sc. C. Schiwek, Dr. J. Meiners, Dr. C. Würtele, Prof. Dr. S. Schneider
Institut für Anorganische Chemie, Georg-August-Universität Tammannstr. 4, 37077 Göttingen (Germany)
E-mail: sven.schneider@chemie.uni-goettingen.de
M. Sc. M. Förster, Dr. M. Diefenbach, Prof. Dr. M. C. Holthausen
Insitut für Anorganische und Analytische Chemie
Goethe-Universität, Max-von-Laue-Str. 7
60438 Frankfurt am Main (Germany)
E-mail: max.holthausen@chemie.uni-frankfurt.de

Supporting information for this article is available on the WWW under http://dx.doi.org/10.1002/anie.201504369.

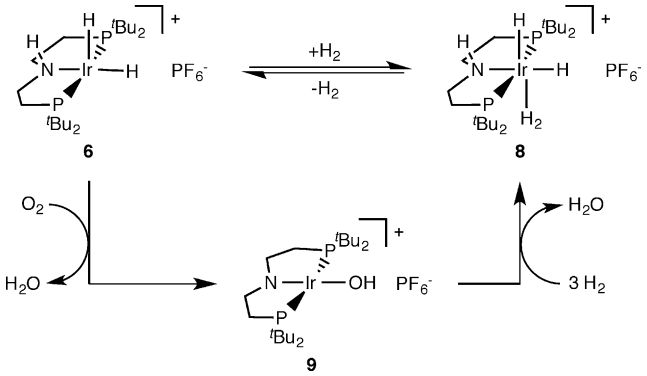

Scheme 2. Synthetic ORR cycle with a bifunctional Ir dihydride.

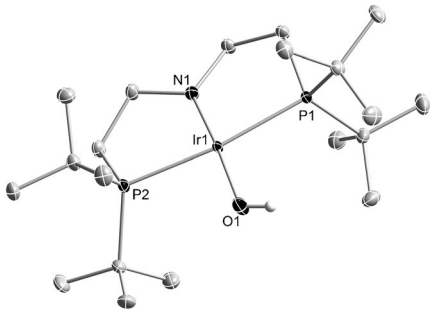

Figure 1. Molecular structure of $[Ir(OH)(PNP)]PF_6$ (**9**). ORTEP plot of the cation with ellipsoids at 50% probability (C–H hydrogen atoms and PF_6^- anion are omitted for clarity). Selected bond lengths [Å] and angles [°]: Ir1–P1 2.3258(5), Ir1–P2 2.3216(5), Ir1–N1 1.8649(16), Ir1–O1 1.9568(14); N1-Ir1-O1 176.58(6), N1-Ir1-P2 84.92(5), O1-Ir1-P2 91.77(5), N1-Ir1-P1 85.27(5), O1-Ir1-P1 98.03(5), P2-Ir1-P1 170.181(16).

Five-coordinate dihydride **6** readily reacts with O_2 (1 bar) at RT (Scheme 2). Full conversion over 30 minutes was observed to a diamagnetic product in up to 85% spectroscopic yield. Isolation and characterization revealed the formation of hydroxy amido complex $[Ir(OH)(PNP)]PF_6$ (**9**). An equimolar amount of water and no indication for H_2O_2 were found upon trap-to-trap transfer of the volatiles after full conversion. Exclusive formation of $[Ir(^{18}OH)(PNP)]PF_6$ with $^{18}O_2$ and therefore O_2 as oxygen source was confirmed by electrospray mass spectrometry. Furthermore, complex **6** does not react with degassed water at room temperature, ruling out hydrolysis as pathway. However, addition of water to the reaction results in higher selectivity of **9** vs. altogether four unidentified para- (^{1}H NMR: 10.2 and 6.1 ppm) and diamagnetic (^{31}P NMR: 63.2 and 62.9 ppm) side products, respectively (see Figures S19/S20 in the Supporting Information).

The full synthetic cycle for ORR is completed by hydrogenolysis of **9** with H_2, which restores the hydride complexes **8**/**6** in around 90% yield (Figure S17) and a second equivalent of water (Scheme 2). Up to three successive O_2-splitting/hydrogenation cycles were run with the same sample at room temperature in CD_2Cl_2 (1 bar O_2 and H_2, respectively). Simultaneous catalyst degradation is mainly attributed to chlorination of **6** by the solvent.[9,10]

The structure of complex **9** was confirmed by spectroscopic characterization and single-crystal X-ray diffraction (Figure 1). A band at 3604 cm^{-1} in the IR spectrum is attributed to the O–H stretching vibration. A broadened ^{1}H NMR peak at 11.6 ppm, which disappears upon addition of D_2O, can be assigned to the OH moiety. Interestingly, the Ir hydroxy complexes reported by Piers and co-workers, $[Ir(OH)\{=C(C_6H_4PR_2)_2\}]$ (R = *i*Pr, *t*Bu; $\delta_{O\text{-}H} = 4.3$ ppm), and Burger and co-workers, $[Ir(OH)\{NC_5H_3(2,6\text{-}C(Me)NR)_2\}]$ (R = 2,6-$Me_2C_6H_3$, 2,6-$iPr_2C_6H_3$; $\delta_{O\text{-}H} = 8.1$ ppm), also exhibit pronounced downfield shifts of the hydroxy protons, for example, in comparison to Milstein's $[Ir(OH)(Ph)\{NC_5H_3(CHPtBu_2)(CH_2PtBu_2)\}]$ ($\delta_{O\text{-}H} = -3.5$ ppm).[5,11] The OH chemical shift of **9** is almost independent on concentration ($\Delta\delta_{O\text{-}H} = 0.07$ ppm at [**9**] = 2–14 mM) ruling out substantial aggregation through OH hydrogen bonding. Further information is provided by variable-temperature NMR spectroscopy. At RT, NMR data of complex **9** are in agreement with C_{2v} symmetry. However, upon cooling, two ^{31}P NMR signals with mutual *trans* coupling ($^2J_{PP} = 336$ Hz) are observed, consistent with hindered rotation of a bent hydroxide ligand at low T ($\Delta^{\ddagger}H = 9.8 \pm 0.3$ kcal mol^{-1}, $\Delta^{\ddagger}S = -1.2 \pm 0.5$ cal $mol^{-1}\,K^{-1}$). The barrier implies HO→Ir π bonding, which is confirmed by DFT computations. In analogy, hindered methoxide rotation was also found for model complex $[Ir(OMe)\{NC_5H_3(2,6\text{-}C(Me)NH)_2\}]$ and attributed to a N–Ir–O 3-center-4-electron π interaction.[11a,12] The NCH_2 ^{1}H NMR signal at −2.23 ppm indicates electronic similarities of **9** also with square-planar iridium alkylidene complexes: A comparable high-field shift of the α-CH_2 group (−2.77 ppm) was reported for Shaw's $[IrCl\{=C(CH_2CH_2PtBu_2)_2\}]$ and attributed to shielding by strong contribution of the ylidic $\{Ir^+-C^-\}$ bond representation.[13] The bonding parameters in the solid state further underline the relevance of N–Ir–O π bonding: The pincer nitrogen atom exhibits planar coordination (sum of angles around N1: 360.0°) and the short Ir1–N1 distance (1.8649(16) Å) indicates N→Ir double bond character, in analogy to divinylamido complex $[IrCl(PNP^*)]PF_6$ ($PNP^* = N(CHCHPtBu)_2$; Ir–N: 1.922(2) Å).[14,15] The Ir1–O1 bond distance (1.9568(14) Å) of **9** is identical with that of Burger's hydroxy complex (1.951(3) Å).[11a] Crystal packing of **9** reveals the absence of OH hydrogen bonding with the PF_6 anion.

Isolable, square-planar 4/5d^6 complexes are exceedingly rare. Ru^{II} complexes $[RuCl(PNP^*)]$ and $[RuCl\{N(SiMe_2CH_2PtBu_2)_2\}]$ exhibit intermediate spin ($S = 1$) ground states,[16] while $[RuCl(PNP)]$ and $[IrCl(PNP^*)]^+$ adopt low-spin ($S = 0$) configurations.[14,17] DFT computations for **9** confirm that the singlet state is favored by $\Delta G = 18.5$ kcal mol^{-1} over the triplet state and the computed structural parameters for $S = 0$ are in good agreement with the X-ray diffraction results. The Ir–N ($S = 0$: 1.887 Å; $S = 1$: 1.992 Å) bond length is particularly sensitive to the spin multiplicity. This observation is in line with the fact that the LUMO ($S = 0$) represents the highest (π*)MO of the N–Ir–O 3-center-4-electron π interaction (Figure 2). The singlet ground state is stabilized by N→Ir π donation, which raises the vacant d_{yz} orbital in energy. Likewise, the coplanar

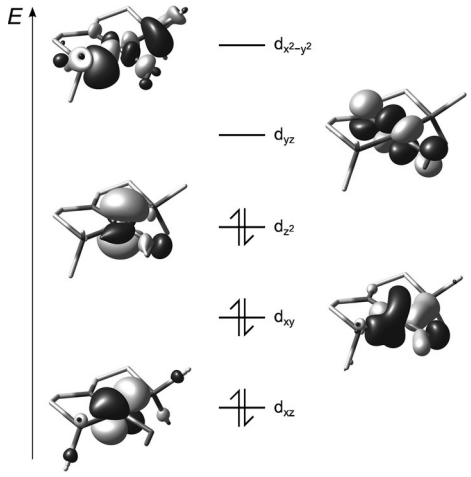

Figure 2. Qualitative FMO diagram for the PMe_2 model system of complex **9** (MO isosurfaces plotted at $0.05\ a_0^{-3/2}$) from DFT computations (RI-PBE-D3/def2-SVP(MWB60)).

arrangement of the Ir–O–H and Ir(PNP) moieties in the singlet minimum conformation enables O→Ir π bonding. Accordingly, at standard conditions an Ir–OH rotational barrier of $\Delta^{\ddagger}H = 12.4\ \text{kcal mol}^{-1}$ was computed, in good agreement with the experimental value (cf. the Supporting Information).

Several pathways were proposed for the oxygenation of group 9 and 10 hydride complexes.[18,19] M–H bond cleavage prior to O_2 splitting results in metal hydroperoxides as the crucial intermediates,[20] which have been isolated occasionally.[6,21] In some cases, dioxygen M–H insertion was attributed to radical mechanisms, like autoxidation[21a,b,22] or hydrogen atom abstraction,[6b,23] while other hydrides undergo peroxide protonation after HX (X = halide, carboxylate) elimination and O_2 coordination.[7,24] Therefore, several mononuclear pathways for the formation of **9** via hydroperoxide intermediates were considered (Scheme 3): a radical chain mechanism (A), hydrogen atom abstraction (HAA) and radical recombination (B), initial H_2 reductive elimination (C), initial N–H/Ir–H H_2 elimination (D), or O_2 coordination/insertion (E).

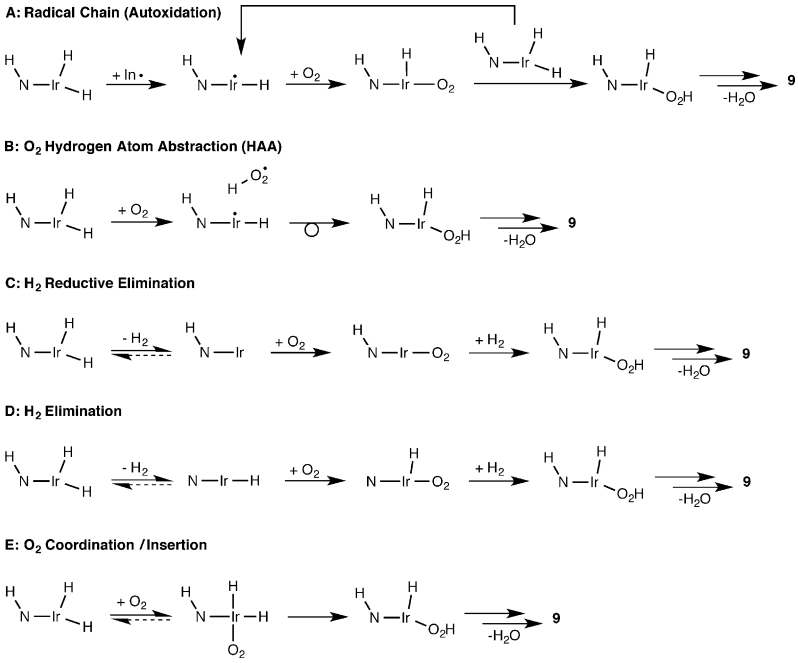

Scheme 3. Possible mechanisms for the conversion of **6** to **9** via a putative hydroperoxide intermediate.

Feller et al. recently described the NMR spectroscopic detection of a putative peroxo intermediate at low *T* during oxygenation of an iridium(I) pincer complex.[5] Monitoring the reaction of **6** and O_2 at 1 and 6 bar, respectively, from −70 °C to RT by NMR spectroscopy reveals onset for the formation of **9**, the diamagnetic side products and some **8** above around −50 °C. However, no intermediates attributable to O_2 binding are observed. Further mechanistic insight was obtained by kinetic analysis (see the Supporting Information). First-order dependence in both **6** and O_2 (with zero *y* intercept) is found for the decay of **6**, according to the simple rate law: $r = k_{obs}\ [\mathbf{6}]$ ($k_{obs} = k_1\ [O_2]$; $k_1 = 0.39 \pm 0.01\ \text{L mol}^{-1}\text{s}^{-1}$). This result allows for an estimate of an overall kinetic barrier around $20\ \text{kcal mol}^{-1}$. Importantly, while added water affects the selectivity in **9** (see above) the decay rate of **6** remains invariant, which implies that the selectivity is determined after the rate-determining step. Furthermore, first-order dependence in **6** provides no indication for bimetallic O_2 activation as suggested in case of monohydride **1**.[2a,3,25] The first-order dependence on O_2 and the rate independence on added radical starter (AIBN) rule out a radical-chain mechanism (A). The oxygenation of $[Ir(D)_2(\textit{H}PNP)]^+$ (D_2-**6**) indicated no H/D kinetic isotope effect (KIE) at variance with what would be expected for an HAA mechanism (B).[26] For pathway C, irreversible H_2 loss should result in rate independence on O_2,[27,21c] while an equilibrium isotope effect (EIE) would be likely for an H_2 reductive elimination pre-equilibrium. Notably, such an EIE could be quenched as a result of the inverse temperature dependence of the zero-point energy contribution vs. the other contributions.[28] However, an H_2 reductive elimination pre-equilibrium is unlikely because in the absence of O_2 solutions of **6** in benzene are stable at RT over an extended time. Pathway D was probed by selective amine H/D labeling: $[Ir(H)_2(\textit{D}PNP)]^+$ (D_1-**6**) also does not exhibit an H/D isotope effect.[29,30] Furthermore, neither $[Ir(D)_2(\textit{H}PNP)]^+$ (D_2-**6**) nor $[Ir(H)_2(\textit{D}PNP)]^+$ (D_1-**6**) undergo H/D scrambling of the hydride and amine protons indicating that H_2 elimination is too slow.

Hence, the kinetic experiments provide no indication for pathways involving dinuclear iridium intermediates. Instead, the rate law together with the absence of detectable intermediates as well as H/D isotope effects favor an O_2

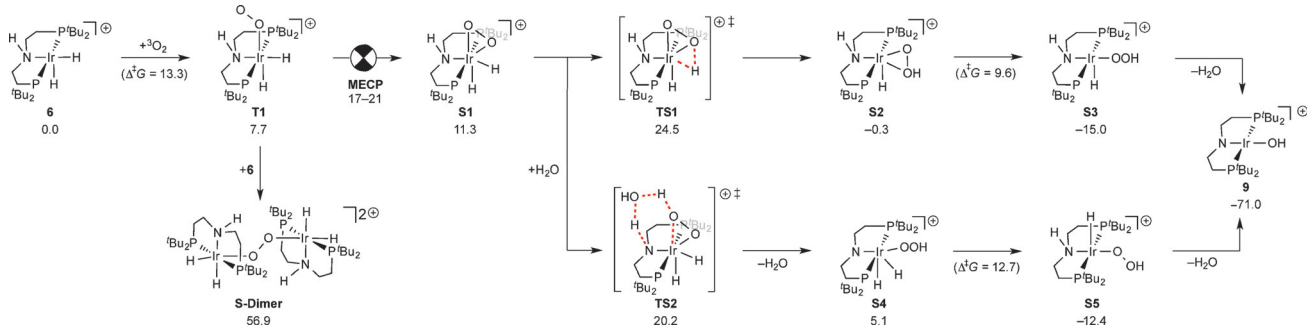

Figure 3. Computed O_2 activation steps (cf. the Supporting Information for a full presentation). ΔG values in kcal mol^{-1} at standard conditions calculated at the RI-PBE-D3/def2-TZVPP(MWB60)//RI-PBE-D3/def2-SVP(MWB60) level of DFT.

coordination/insertion pathway (E) with rate-limiting O_2 binding. These interpretations find strong support from DFT computations[31,32] conducted in detail for the kinetically relevant O_2 activation steps up to hydroperoxide formation. Overall, formation of **9** and water from **6** and O_2 is strongly exergonic with $\Delta G = -71$ kcal mol^{-1}. Initial dinuclear bridging peroxide formation is excessively endergonic (Figure 3). Instead, the lowest energy pathway resulting from a detailed assessment of paths B–E corresponds to an O_2-coordination/insertion route (E): Binding of O_2 to **6** results in the initial formation of triplet superoxo complex **T1**. Side-on peroxo complex **S1** is accessible after transition from the triplet to the singlet surface,[33] for which the corresponding minimum energy crossing point (MECP) was located.[34] Considering rough estimates for the free-energy correction and a surface crossing probability smaller than unity (Supporting Information), we arrive at a kinetic barrier for the transition from **T1** to **S1** in the range of 17–21 kcal mol^{-1}.[35] Subsequent H-shift via **TS1** (25 kcal mol^{-1}) yields side-on hydroperoxide intermediate **S2**, which isomerizes to the more stable end-on analog **S3** with moderate barrier.

Motivated by the experimentally observed selectivity increase upon water addition, we investigated the effect of water assisted H-atom transfer to the peroxo ligand. While the effective barrier for hydride transfer remains equally high (Supporting Information), the N–H proton transfer is catalyzed by water (**TS2**). With subsequent liberation of water and low-barrier Ir–H reductive elimination to N, this path provides a lower effective barrier from **S1** to **S5** (20 kcal mol^{-1}). Hence, the computed barriers for the MECP and **TS2** are in a similar range and both are in good agreement with our kinetic estimate. Importantly, the absence of an N–H/D KIE in the experiments with added H_2O/D_2O indicates that the reaction rate is not determined by the proton shift (computed H/D KIE for **TS2**: 8.39) but by the preceding spin surface crossing near the MECP.[36]

In conclusion, we present an iridium dihydrido complex that formally catalyzes the ORR of O_2 with H_2 within several synthetic cycles. Four-electron O_2 splitting is accompanied by hydride oxidation of **6** and formation of the highly unusual, square-planar Ir^{III} complex **9**. Preliminary experimental and computational mechanistic data on the oxygen activation step point towards mononuclear, intramolecular four-electron O_2 reduction with rate-determining O_2 binding followed by a H-transfer. Theory suggests spin-surface crossing phenomena acting as a kinetic bottleneck. Further, the presence of catalytic amounts of water is indispensable to explain efficient hydroperoxide formation. Therefore, the PNP pincer ligand seems to be "bifunctional" in a sense that it serves as proton relay and stabilizes **9** through N→Ir π donation.

Acknowledgements

We are grateful to the Deutsche Forschungsgemeinschaft (Emmy Noether Programm SCHN950/2) and the COST action CM1205 (CARISMA) for support. Quantum chemical calculations have been performed at the Center for Scientific Computing (CSC) Frankfurt on the FUCHS and LOEWE-CSC high-performance compute clusters.

Keywords: density functional calculations · hydrides · iridium · oxygen · pincer ligands

How to cite: *Angew. Chem. Int. Ed.* **2015**, *54*, 15271–15275
Angew. Chem. **2015**, *127*, 15486–15490

[1] L. Que, Jr., W. B. Tolman, *Nature* **2008**, *455*, 333.
[2] Representative examples: a) Z. M. Heiden, T. B. Rauchfuss, *J. Am. Chem. Soc.* **2007**, *129*, 14303; b) D. K. Dogutan, S. A. Stoian, R. McGuire, Jr., M. Schwalbe, T. S. Teets, D. G. Nocera, *J. Am. Chem. Soc.* **2011**, *133*, 131; c) C. T. Carver, B. D. Matson, J. Mayer, *J. Am. Chem. Soc.* **2012**, *134*, 5444; d) J. T. Henthorn, S. Lin, T. Agapie, *J. Am. Chem. Soc.* **2015**, *137*, 1458.
[3] S. Chowdhury, F. Himo, N. Russo, E. Sicilia, *J. Am. Chem. Soc.* **2010**, *132*, 4178.
[4] Owing to the high covalency of late transition metal M–H bonds the formal oxidation state is not a good descriptor for charge.
[5] M. Feller, E. Ben-Ari, Y. Diskin-Posner, R. Carmieli, L. Weiner, D. Milstein, *J. Am. Chem. Soc.* **2015**, *137*, 4634.
[6] Representative examples: a) M. M. Konnick, B. A. Gandhi, I. A. Guzei, S. S. Stahl, *Angew. Chem. Int. Ed.* **2006**, *45*, 2904; *Angew. Chem.* **2006**, *118*, 2970; b) M. C. Denney, N. A. Smythe, K. L. Cetto, R. A. Kemp, K. I. Goldberg, *J. Am. Chem. Soc.* **2006**, *128*, 2508.
[7] D. B. Williams, W. Kaminsky, J. M. Mayer, K. I. Goldberg, *Chem. Commun.* **2008**, 4195.
[8] J. Meiners, A. Friedrich, E. Herdtweck, S. Schneider, *Organometallics* **2009**, *28*, 6331.
[9] Note that complex **9** is not soluble in non-polar hydrocarbons, such as benzene. Furthermore, THF is oxygenated to γ-

butyrolactone in the presence of **6** and O_2, as reported for Vaska's complex.[10]

[10] C. Tejel, M. A. Ciriano, *Top. Organomet. Chem.* **2007**, *22*, 97.

[11] a) D. Sieh, M. Schlimm, L. Andernach, F. Angersbach, S. Nückel, J. Schöffel, N. Šušňjar, P. Burger, *Eur. J. Inorg. Chem.* **2012**, 444; b) R. J. Burford, W. E. Piers, D. H. Ess, M. Parvez, *J. Am. Chem. Soc.* **2014**, *136*, 3256.

[12] S. Nückel, P. Burger, *Organometallics* **2001**, *20*, 4345.

[13] D. Empsall, E. M. Hyde, R. Markham, W. S. McDonald, M. C. Norton, B. L. Shaw, W. Weeks, *J. Chem. Soc. Chem. Commun.* **1977**, 589.

[14] J. Meiners, M. G. Scheibel, M.-H. Lemée-Cailleau, S. A. Mason, M. B. Boeddinghaus, T. F. Fässler, E. Herdtweck, M. M. Khusniyarov, S. Schneider, *Angew. Chem. Int. Ed.* **2011**, *50*, 8184; *Angew. Chem.* **2011**, *123*, 8334.

[15] S. Schneider, J. Meiners, B. Askevold, *Eur. J. Inorg. Chem.* **2012**, 412.

[16] a) L. A. Watson, O. V. Ozerov, M. Pink, K. G. Caulton, *J. Am. Chem. Soc.* **2003**, *125*, 8426; b) B. Askevold, M. M. Khusniyarov, W. Kroener, K. Gieb, P. Müller, E. Herdtweck, F. W. Heinemann, M. Diefenbach, M. C. Holthausen, V. Vieru, L. F. Chibotaru, S. Schneider, *Chem. Eur. J.* **2015**, *21*, 579.

[17] B. Askevold, M. M. Khusniyarov, E. Herdtweck, K. Meyer, S. Schneider, *Angew. Chem. Int. Ed.* **2010**, *49*, 7566; *Angew. Chem.* **2010**, *122*, 7728.

[18] a) A. N. Campbell, S. S. Stahl, *Acc. Chem. Res.* **2012**, *45*, 851; b) L. Boisvert, K. I. Goldberg, *Acc. Chem. Res.* **2012**, *45*, 899; c) M. L. Scheuermann, K. I. Goldberg, *Chem. Eur. J.* **2014**, *20*, 14556.

[19] Most recently, a mechanism via Ir^{IV} oxo species was proposed for oxygenation of an iridium methyl complex: M. C. Lehman, D. R. Pahl, J. M. Meredith, R. D. Sommer, D. M. Heinekey, T. R. Cundari, E. A. Ison, *J. Am. Chem. Soc.* **2015**, *137*, 3574.

[20] M. T. Atlay, M. Preece, G. Strukul, B. R. James, *J. Chem. Soc. Chem. Commun.* **1982**, 406.

[21] a) A. Bakac, *J. Am. Chem. Soc.* **1997**, *119*, 10726; b) D. D. Wick, K. I. Goldberg, *J. Am. Chem. Soc.* **1999**, *121*, 11900; c) T. S. Teets, D. G. Nocera, *J. Am. Chem. Soc.* **2011**, *133*, 17796.

[22] J. L. Look, D. D. Wick, J. M. Mayer, K. I. Goldberg, *Inorg. Chem.* **2009**, *48*, 1356.

[23] a) J. M. Keith, R. P. Muller, R. A. Kemp, K. I. Goldberg, W. A. Goddard III, J. Oxgaard, *Inorg. Chem.* **2006**, *45*, 9631; b) J. M. Keith, T. S. Teets, D. G. Nocera, *Inorg. Chem.* **2012**, *51*, 9499.

[24] a) B. V. Popp, S. S. Stahl, *J. Am. Chem. Soc.* **2007**, *129*, 4410; b) M. M. Konnick, S. S. Stahl, *J. Am. Chem. Soc.* **2008**, *130*, 5753; c) N. Decharin, B. V. Popp, S. S. Stahl, *J. Am. Chem. Soc.* **2011**, *133*, 13268; d) T. S. Teets, D. G. Nocera, *Inorg. Chem.* **2012**, *51*, 7192.

[25] Note that slow formation of an O_2 adduct of **6** and subsequent rapid, irreversible trapping by another equivalent of **6** could also exhibit first-order kinetics in **6**.

[26] Complex D_2-**6** undergoes slow scrambling of the deuteride ligands with the *t*Bu C–H groups. However, the timescale of this process is considerably slower ($t_{1/2} = 45$ min) than the reaction with O_2 under the conditions of the kinetic examinations; $p(O_2) = 6$–11 bar.

[27] A related iridium(III) peroxo complex was reported: M. Kinauer, M. G. Scheibel, J. Abbenseth, F. W. Heinemann, P. Stollberg, C. Würtele, S. Schneider, *Dalton Trans.* **2014**, *43*, 4506.

[28] G. Parkin, *Acc. Chem. Res.* **2009**, *42*, 315.

[29] The N–H/D KIE was derived in the presence of added H_2O and D_2O, respectively, to prevent H/D scrambling with formed water (see the Supporting Information).

[30] V. I. Bakhmutov, *Eur. J. Inorg. Chem.* **2005**, 245.

[31] DFT computations were performed at the RI-PBE-D3/def2-TZVPP(MWB60)//RI-PBE-D3/def2-SVP(MWB60) level of theory. The quality of the results was confirmed by CCSD(T)-F12b reference calculations (see the Supporting Information).

[32] We limit our assessment to the LS coupling scheme, as a rigorous treatment of spin–orbit coupling effects (SOC) is beyond the scope of the present investigation. Note that this approach is frequently used for 5d transition metals, even though a *J*„*J*-coupling scheme might be necessary for a quantitative treatment. See, for example, ref. [3].

[33] For a theoretical assessment of superoxo/peroxo isomerizations see H. Yu, Y. Fu, Q. Guo, Z. Lin, *Organometallics* **2009**, *28*, 4443.

[34] J. N. Harvey, M. Aschi, H. Schwarz, W. Koch, *Theor. Chem. Acc.* **1998**, *99*, 95.

[35] The surface crossing probability is governed by the spin – orbit coupling strength and the topology of the isoenergetic path shared between the two spin surfaces along the reaction coordinate, which reduces the surface crossing probability. This affects kinetic barriers derived from MECP energies; proficient estimates for the corresponding, additional energy increase amount to $1-5\ \mathrm{kcal\,mol^{-1}}$ for relevant related cases, see J. N. Harvey, *Phys. Chem. Chem. Phys.* **2007**, *9*, 331 and J. N. Harvey, *WIREs Comput. Mol. Sci.* **2014**, *4*, 1.

[36] a) K.-B. Cho, H. Chen, D. Janarnan, S. P. de Visser, S. Shaik, W. Nam, *Chem. Commun.* **2012**, *48*, 2189; b) R. Prabhakar, P. E. M. Siegbahn, B. F. Minaev, H. Ågren, *J. Phys. Chem. B* **2004**, *108*, 13882.

Received: May 13, 2015
Revised: September 7, 2015
Published online: October 29, 2015

